Supplement of Solid Earth, 14, 937–959, 2023
https://doi.org/10.5194/se-14-937-2023-supplement

Solid Earth Open Access EGU

Supplement of

Numerical modeling of stresses and deformation in the Zagros–Iranian Plateau region

Srishti Singh and Radheshyam Yadav

Correspondence to: Radheshyam Yadav (shamgpbhu@gmail.com)

Supplement

Contents of this file

- Figures S1 to S3
- Tables S1 to S2

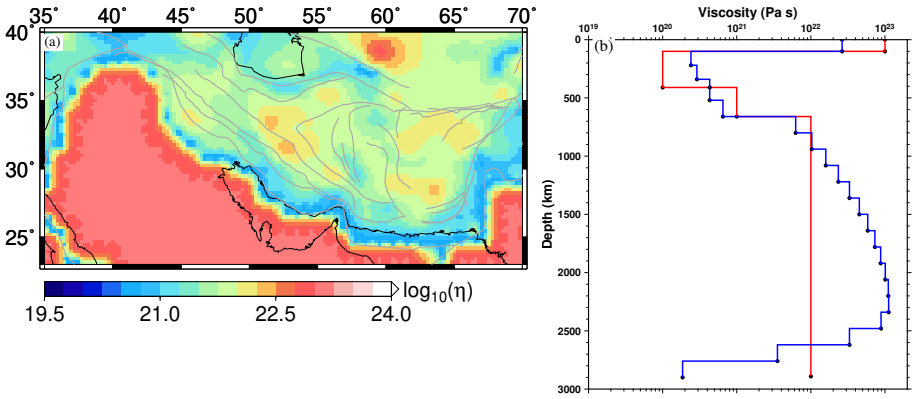

Figure S1. (Left) Plot of lithospheric viscosity in the study region that is used in finite element models. Right panel shows GHW13(red) (Ghosh et al., 2013) and SH08 (blue) (Steinberger and Holme, 2008) viscosity structures used in mantle convection models.

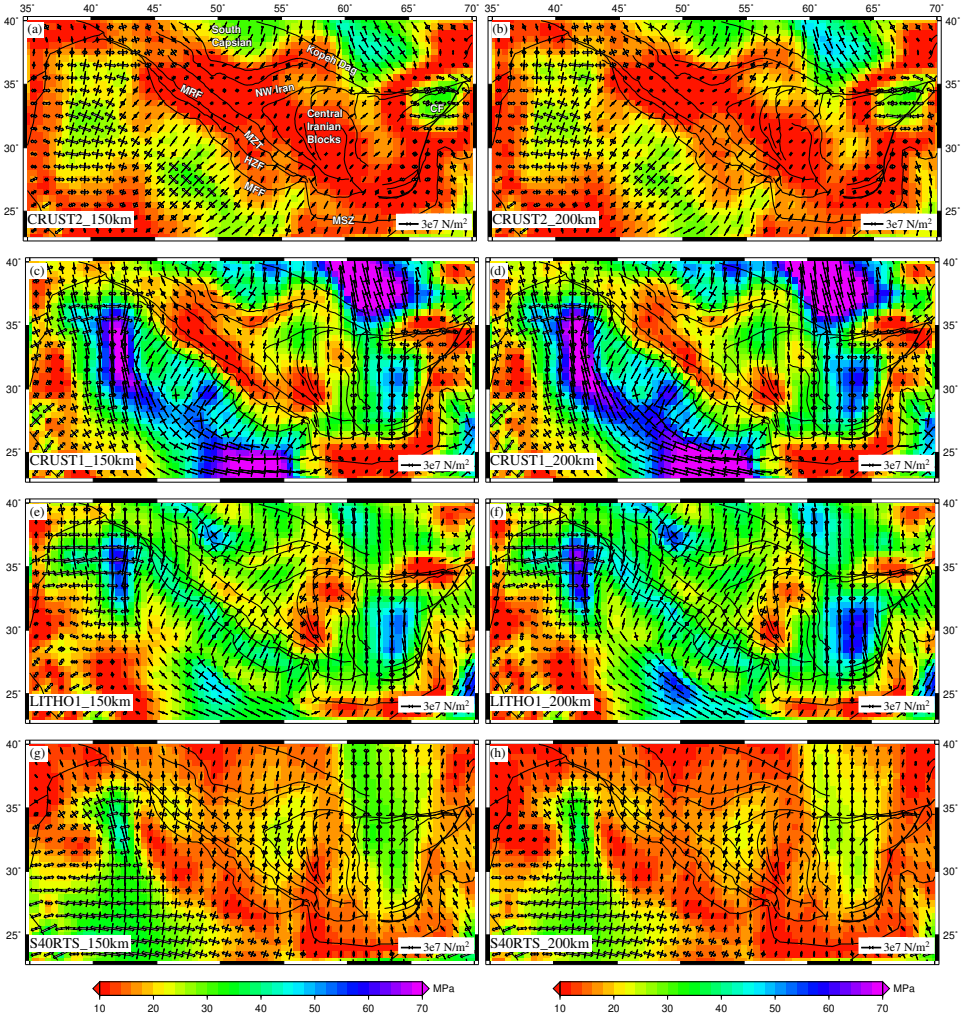

Figure S2. (a-f)Deviatoric stresses predicted using GPE models for lithosphere base at 150 km (left) and 200 km (right). (g-h) Mantle derived stresses from S40RTS tomography model for GHW13 viscosity structures, when LAB is at 150 km (left) and 200 km (right). The background plot shows the second invariant of deviatoric stresses. The white arrows denote tensional stresses, and black arrows indicate compressional stresses.

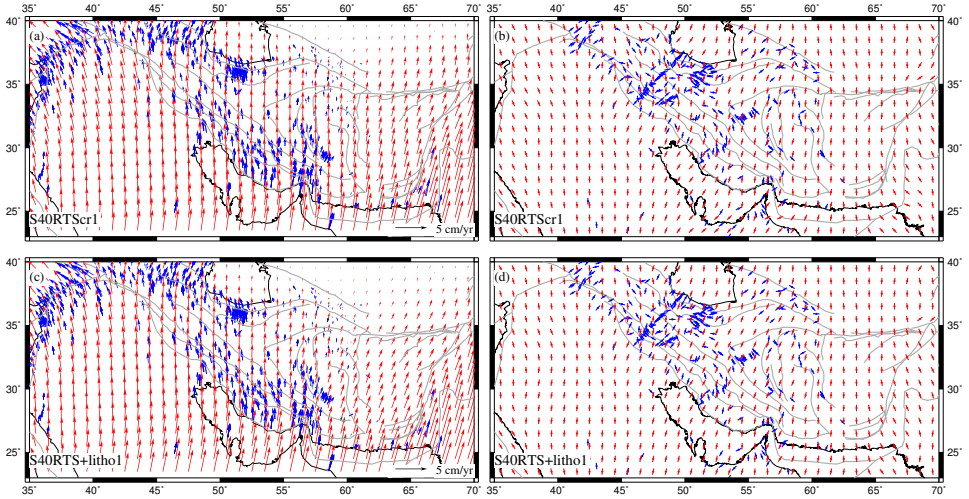

Figure S3. (Left Panel) GPS (blue) and predicted (red) plate velocities with respect to a fixed Eurasian plate. Right Panel shows plot of FPDs in blue and S_{Hmax} in red.

Table S1. Summary of quantitative comparison of predicted results of various models with observed data for SH08 viscosity model (Steinberger and Holme, 2008).

Model	S_{Hmax} **misfit**	**Strain rate correlation**	**RMS error (mm/yr)**	**Angular misfit**	**Total error**
S40RTS+SH08	0.58	0.90	5.68	6.00	2.42
SAW642AN+SH08	0.58	0.88	17.41	22.00	3.56
3D2018_S40RTS+SH08	0.58	0.88	8.68	9.20	2.86
S2.9_S363+SH08	0.54	0.89	10.38	14.00	2.99
S40RTS+SH08cr2	0.52	0.91	3.81	3.30	1.95
SAW642AN+SH08cr2	0.56	0.89	5.38	5.10	2.35
3D2018_S40RTS+SH08cr2	0.54	0.89	4.15	3.30	2.07
S2.9_S362+SH08cr2	0.52	0.92	5.14	5.80	2.24
S40RTS+SH08cr1	0.54	0.92	4.80	6.10	2.19
SAW642AN+SH08cr1	0.54	0.91	8.61	10.70	2.78
3D2018_S40RTS+SH08cr1	0.56	0.91	6.30	7.90	2.49
S2.9_S362+SH08cr1	0.55	0.91	5.82	7.60	2.40
S40RTS+SH08+litho	0.52	0.94	5.79	7.40	2.34
SAW642AN+SH08+litho	0.51	0.94	8.05	8.70	2.66
3D2018_S40RTS+SH08+litho	0.53	0.94	6.61	8.20	2.48
S2.9_S362+SH08+litho	0.53	0.94	7.61	10.10	2.62

Model/LAB Depth	S_{Hmax} error			Strain Rates Correlation			Velocity rms error		
	100 km	150 km	200 km	100 km	150 km	200 km	100 km	150 km	200 km
CRUST2	0.77	0.64	0.60	0.69	0.83	0.87	7.32	5.85	5.69
CRUST1	0.64	0.61	0.60	0.87	0.9	0.9	7.44	8.59	9.28
LITHO1	0.59	0.56	0.56	0.92	0.93	0.93	8.51	9.03	9.45
S40RTS	0.57	0.56	0.54	0.88	0.89	0.90	6.20	5.90	6.06
S40RTScr2	0.48	0.48	0.49	0.92	0.92	0.93	3.28	5.24	3.82
S40RTScr1	0.51	0.52	0.53	0.92	0.92	0.92	4.29	9.60	9.28
S40RTS+litho1	0.49	0.50	0.51	0.93	0.93	0.94	4.52	9.03	9.45

Table S2. Quantitative comparison of fit to the observed data for varying LAB depths.

References

Ghosh, A., Holt, W. E., and Wen, L.: Predicting the lithospheric stress field and plate motions by joint modeling of lithosphere and mantle dynamics, Journal of Geophysical Research: Solid Earth, 118, 346–368, 2013.

Steinberger, B. and Holme, R.: Mantle flow models with core-mantle boundary constraints and chemical heterogeneities in the lowermost mantle, Journal of Geophysical Research: Solid Earth, 113, https://doi.org/10.1029/2007JB005080, 2008.